Designing and Initial Testing of a Tyre Strain Sensing System to Estimate Slip in Robotic Platforms

Ali Farooq Lutfi Lutfi[1,2], Tobias Low[1], Andrew Maxwell[1]
[1]Faculty of Health, Engineering and Sciences, University of Southern Queensland, Toowoomba, Australia
[2]Control and Systems Engineering Department, University of Technology, Baghdad, Iraq
{AliFarooqLutfi.Lutfi, Tobias.Low, Andrew.Maxwell}@usq.edu.au

Abstract

Wheel slip estimation is an important element in improving the performance of wheeled mobile robots. Conventional wheel slip estimation methods relied upon sensors which were far from the tyre-ground interface; hence, they required the use of approximated models and complex transformations. A modern method, which directly measures tyre-ground contact quantities utilising in-tyre sensors, helps develop accurate and direct wheel slip estimation techniques. The work presented in this paper represents a first stage towards developing such techniques. An optimum sensing system for a small, non-pressurised robot's tyre is presented. Experimental work is conducted to determine the possibility of bonding the selected system inside the tyre. Static footprint tests are undertaken to derive an optimal design for the sensing system. Image processing is utilised to obtain dimensions of the tyre-ground contact patches provided by these tests. Performance of the produced system design is evaluated with static tests using a custom-built, bench-top rig. Results of these tests demonstrated a sufficient degree of consistency in the measurements of the sensory system. In addition, the strain profiles extracted from the sensors' readings agree with key theoretical facts.

1 Introduction

Wheel slip represents a determinant factor in a number of applications for wheeled mobile robots. First, odometric solutions produce false position estimations during wheel slip incidents [Chae and Song, 2013]. In addition, taking wheel slip into consideration is a crucial element in developing efficient path planning algorithms [Ward and Iagnemma, 2008]. Moreover, wheel slip estimation is a key component in enhancing various control systems, such as traction control and stability control [Song *et al.*, 2008]. Also, wheel slip affects the navigation of the mobile robot and hinders its performance in target chasing and obstacle avoidance. Furthermore, as it does not contribute to the desired robot motion in the planned path, wheel slip is regarded as a form of energy loss. Thus, wheel slip estimation results in a reduction of the robot's energy consumption.

Conventional wheel slip estimation methods based on different sensors such as accelerometers, gyros, IMU, and cameras have been proposed [Yi *et al.*, 2009; Song *et al.*, 2008; Chae and Song, 2013]. These sensors were mounted on different positions on the body of the robot. Hence, to interpret the indirect measurements collected by these sensors about the tyre-ground dynamic events, a number of projections from one coordinate system to another as well as imprecise mathematical models were required [Krier *et al.*, 2014]. Additionally, some of the issues which are encountered with cameras, which are the main competing sensors for slip detection in mobile robots, are the necessity of identifying traceable features as well as the known defects of cameras such as illumination problems and images' disturbances caused by dynamic obstacles in the scene [Chae and Song, 2013; Ward and Iagnemma, 2008]. However, because of developing sensor technologies, it is possible now to embed various types of sensors in the tyre to directly measure different tyre-ground quantities [Palmer *et al.*, 2002].

It is argued that a significant improvement to wheel slip estimation approaches could be achieved by developing in-tyre sensory systems. The reason is that tyres produce nearly all forces and moments experienced by the vehicle [Tuononen, 2008]. To estimate these quantities, a tyre being converted into a sensing unit outperforms other solutions in terms of direct detection of variations, high robustness, and close proximity to the interface area. Moreover, Erdogan *et al.* [2011] suggested that tyre sensors can deliver reliable readings even under normal, steady- state driving which is generally not the case with standard sensors. Therefore, utilising such systems, measurements, which are direct, real-time, and

as close to the tyre contact patch as possible could be collected and deployed for accurate wheel slip detection.

This study presents an in-tyre sensing system which can accurately measure tyre-ground interactions for small, non-pressurised robots' tyres. To develop this system, the knowledge gained from both the automotive field and the robotic field will be employed. Experimental work is presented to show possible techniques to mount sensors inside a robot's tyre as well as to study its contact patch. Finally, static tests on a custom-built, bench-top rig are conducted to assess the performance of the implemented sensing system.

2 Identifying Appropriate Sensing System for Robots' Tyres

Tyre Sensing systems previously presented in both the automotive and the robotic fields were examined to identify a suitable sensory solution. In these two fields, the sizes and materials of wheels and tyres are different.

2.1 In the Automotive Field

Since equipping car tyres with sensors, to monitor both the road and tyre conditions, can effectively enhance road safety, several in-tyre sensing systems have been presented in the field of intelligent tyres [Matsuzaki and Todoroki, 2008]. These systems can be divided into non-contacting strain sensing, contacting strain sensing, acceleration sensing, and force sensing systems.

Non-contacting strain sensing systems need no major modifications for the tyre structure. Therefore, they will not affect tyre primary tasks as well as tyre deformation measurements. On the other hand, the most important points to consider are the large sensor size and the need for complex data processing algorithms to model sensor data [Moffitt *et al.*, 2009]. In these systems, the sensing element is not mounted on the tyre; instead, the sensor is attached to the wheel rim inside the tyre to continuously monitor the tyre inner surface. Nearly all non-contacting strain sensing methods are based on optical sensors; however, the use of an acoustic sensor was also noted.

Developed non-contacting, optical sensing systems utilised a position sensitive diode (PSD) [Tuononen, 2008]; CCD camera [Matsuzaki *et al.*, 2012]; or laser sensors [Xiong and Tuononen, 2014]. Clearly, a large space inside the tyre, between the wheel rim and the tyre inner surface, is required to build such systems. Therefore, they are not suitable for small robots' tyres.

It should be mentioned that, non-contacting strain sensing systems based on an ultrasonic sensor has also been used [Magori *et al.*, 1998]. Nevertheless, measurement accuracy was reported to be severely affected by echo attenuations caused by interferences of spurious signals.

With contacting strain sensing systems, direct measurements are acquired. In addition, from a signal processing perspective, strain data are easier to analyse because the strain sensor measures tyre deformations only in its vicinity [Moffitt *et al.*, 2009]. At the same time, these sensors should be flexible enough to follow the tyre rubber elastic characteristics. This ensures that the sensor will capture the local tyre deformations without external disturbances. Also, this compatibility is required to avoid adhesion failure [Matsuzaki and Todoroki, 2008]. Contacting strain sensing depends on a strain sensor mounted on the tyre inner surface [Erdogan *et al.*, 2011; Palmer *et al.*, 2002] or embedded in the tyre rubber [Palmer *et al.*, 2002]. Strain sensors can be placed on the tyre inner surface longitudinally or laterally to detect strain changes in the respective direction.

It is worthwhile to mention that a special approach of strain sensing, a self-sensing technique, where the steel wires in the tyre belts serve as electrodes to indicate capacitance variations was introduced [Matsuzaki and Todoroki, 2008]. This approach can not be adopted for robots' tyres since there are no steel wires integrated into their much simpler structure.

Acceleration sensing systems can provide reliable readings since they can endure sudden measurement peaks when passing through the contact patch. However, a number of challenges are visualised for developing these systems [Ergen *et al.*, 2009; Moffitt *et al.*, 2009]. First, a sophisticated data processing algorithm is crucial to decouple rotational accelerations, gravitational accelerations, and vibration signals.Thus, choosing such sytems to study a dynamic problem as complex as wheel slip will further complicate the matter. Secondly, it was seen that the accelermoeters, used to build these systems by other researchers, are expensive. It is impractical to embed such high-cost components inside the low-cost robots' tyres.

Force sensing systems can measure local forces in the contact patch [Zhang *et al.*, 2013]. Therefore, they can be used to build a better understanding about complex, dynamic events at the tyre-road interface. In spite of this benefit, several negative points are related to these systems. Special manufacturing processes are required to develop these designs [Moffitt *et al.*, 2009]. Also, they can deliver inaccurate sensing because local deformations are easily disturbed by movements of required augmented parts [Ise *et al.*, 2013]. In addition, they need perfect positioning which may not be achieved due to physical constraints. Furthermore, it is a challenging task to measure the contact forces at the tyre-road contact patch due to tyre rubber properties and the highly intercorrelated contact forces in longitudinal, lateral, and normal directions [Zhang *et al.*, 2013].

2.2 In the Robotic Field

For wheeled mobile robots, the few in-wheel sensing systems, which were all dedicated to collect measurements only in the longitudinal direction of motion, can be divided into two groups: wheel deflection sensory systems and tyre rubber deformation sensory systems. Designs in the first group aim at developing sensing modules particularly for planetary rovers, which traverse either loose soil or rugged terrains with a very low speed motion [Iizuka *et al.*, 2014]. Regarding wheel type, measured parameters, and service conditions, this group is neither relevant nor applicable for the specifications of the proposed research. The second class includes especially designed sensors which monitor tyre rubber deformations to extract wheel-ground contact information [Yi, 2008].

In both the automotive and robotic field, it can be concluded that various sensor types, technologies, and configurations were presented to develop tyre deformation sensing systems. Taking into account the cost, complexity, availability, compatibility with tyre material, and size, contacting strain sensing utilising a flexible sensor is suggested for this research. The contacting sensors will be glued on the tyre inner surface as the other option, which is sensors embedded inside the tyre tread, is more difficult to be positioned properly and may not provide useful data due to the relative motion between the sensor and the tyre throughout the contact patch [Zhang *et al.*, 2013].

3 Testing the Possibility of Building a Strain Sensing System Inside a Robot's Tyre

The strain gauges utilised for this research were from Micro-Measurements division (Measurements group, INC.). The gauges type is CEA-06-240UZ-120 Student Gauges. The resistance of the gauge in ohms is $120.0 \pm 0.3\%$ and the gauge factor is $2.070 \pm 0.5\%$ at 24°C. These low-cost, general-purpose, experimentally widely used gauges are extremely thin, 0.056 mm, and flexible. For static strain readings, they operate in a temperature range from $-75°$ to $+175°$C. For single cycle use, these high-elongation gauges can measure up to 5% elongation. To reduce thermal effects to least possible levels, self-temperature compensation (STC) characteristics has been added to the gauges during the production process. All these features make these sensors an ideal solution for developing a sensing system inside a robot's tyre. In this context, it should be affirmed that designing a special sensor is out of the scope of this work. However, designing a new tyre sensing system, in terms of sensors type, number, and configuration, is indispensable to reach the specific research objectives. In the following, the successive stages to bond these sensors on the inner surface of a robot's tyre are described.

Stage 1: Learning how to bond sensors to rubber using a piece of rubber and plastic samples. Many plastic samples were cut to the same size of the strain gauges. The three main steps were surface preparation by cleaning, abrading, and marking; plastic samples' preparation; and bonding operation. The benefit of this stage was choosing appropriate cleaning substances, deciding a suitable grit degree for the abrasive paper, learning how to deal with, transfer, and position the samples, selecting a proper marker, determining type and amount of adhesive, and mastering the bonding process.

Stage 2: Gluing a real strain gauge on a rubber strip utilising experience gained in **Stage 1**. After that, wires were soldered to the gauge. A data acquisition system (DAQ) based on National Instruments hardware and LabVIEW software was built to collect the sensor reading. It consists of NI cDAQ-9172, NI 9219, and LabVIEW 2014. The built-in quarter-bridge configuration of NI 9219 was used. During this simple test, the belt was manually pulled to apply small amount of force and corresponding strain changes were indicated by the sensor output.

Stage 3: Gluing strain gauges on different locations on the inner surface of a robot's tyre. The previously mentioned surface preparation, gauge bonding, and soldering operations were performed to install the sensors inside the tyre. The only new factor introduced to these operations was the curved surface of the tyre inner liner. It significantly increased the complexity of these tasks especially when taking into account that more than one sensor was placed across the limited space of the tyre width.

Robots' tyres are usually fused to the wheel with a very strong adhesive. Since the application of in-tyre sensors requires the ability to easily get the tyres off the wheels, the standard tyres were not helpful and the best solution was to use the so called bead-lock rims. In these wheels, the tyre is fixed to the wheel with a bead-lock ring which is secured using screws to fix the tyre edge to the rim. The tyres are non-pressurised, i.e., they use foam inserts instead of air. This type of tyres is commonly used for robotic platforms. The tyre is about 95 mm in inner diameter, 139 mm in outer diameter, 87 mm in width, and 10 mm in sidewall height.

Stage 4: Building a single-wheel, bench-top test rig to examine the performance of the in-tyre strain sensors using static tests. As can be seen in Figure 1, vertical forces and horizonal forces can be applied on the tyre by means of a slider mechanism. In these initial tests, the tyre was fixed in place such that the in-tyre sensors are at the centre of the contact patch. Different values of vertical and horizontal forces were tested and the corresponding sensors' responses were collected using the

DAQ system. Wires were used to access the data from inside the tyre during the tests.

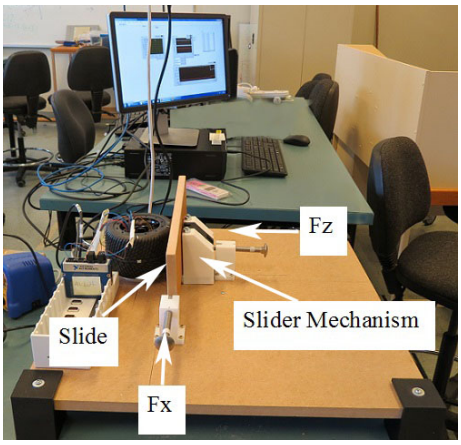

Figure 1: Tyre bench-top rig- Setup for initial tests.

4 Footprint Tests to Examine Tyre Contact Patch

Compression tests were conducted using a compression machine to study the contact patch in terms of its shape (contour) as well as the effect of changing the vertical force on varying its shape and size. Knowing these features will lead to suggesting an optimum design of the sensory system for the particular tyre used herein. Figure 2 shows the experimental setup of these tests. A u-shaped Aluminium bracket was manufactured to hold the tyre in these tests. The bracket makes use of the small screws in the bead-lock rim to fix the tyre from its two sides. A 3D printed part was designed and screwed to the upper side of the bracket to attach the tyre to the compression machine. To obtain the fooprints of the tyre in the tests, a stamp pad was used to smear the lower half of the tyre outer surface with ink. After that, the tyre was pressed vertically against a flat wooden board on which a white paper was taped. Different values of vertical loads were applied starting from the lowest value, where the tyre just begins to make contact with the board, to the maximum value, where it was thought that applying a higher force will damage the tyre or the rim. The range of the vertical loads was between 5N to 100N in increment of 5N.

After completing the tests, the 20 contact patch prints were scanned into computer. The images were processed in Matlab to measure, in pixels, the footprint area, the maximum longitudinal length, and the maximum lateral length. Figure 3 illustrates the steps of the image processing algorithm used to find the required quantities. A spatial calibration factor was then calculated and used to convert these measurements from pixels to millimetres.

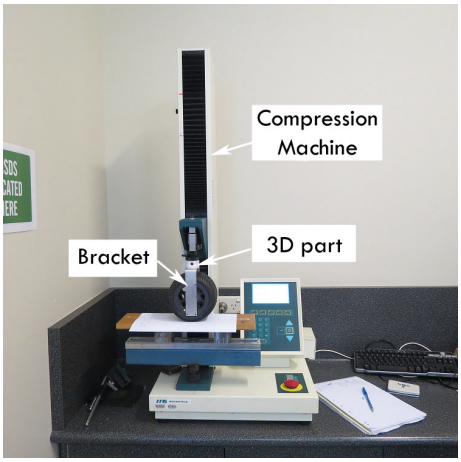

Figure 2: Setup of the footprint tests.

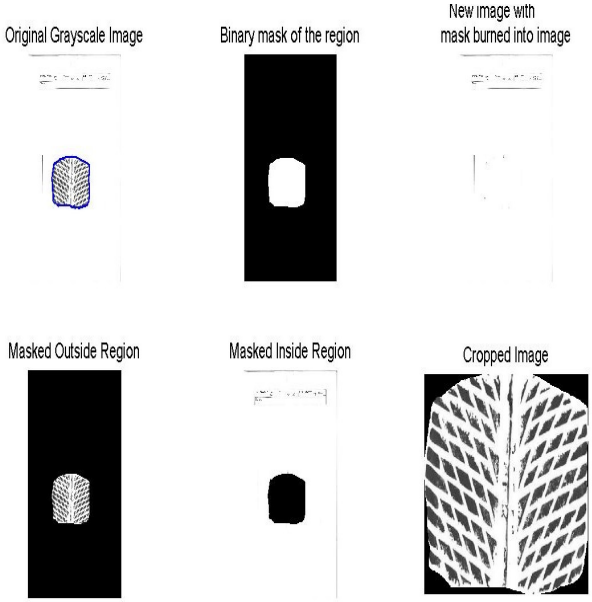

Figure 3: Image processing for the tyre footprint.

It can be seen in Figure 4- Figure 6 that as the vertical force increases, the vertical tyre displacement (vertical tyre deformation) and the footprint geometry increases. However, it can be noticed that starting from vertical force= 60N, the curves almost saturate. Also, the increase in the longitudinal length is more notable than the increase in the lateral length (Figure 6).

5 Sensor System's Design and Placement

5.1 Sensor System's Design

From the results of the static compression tests, it was decided to place the senor system in an area which corresponds to the smallest possible footprint, resulted from a vertical load of 10 N. This engineering decision was

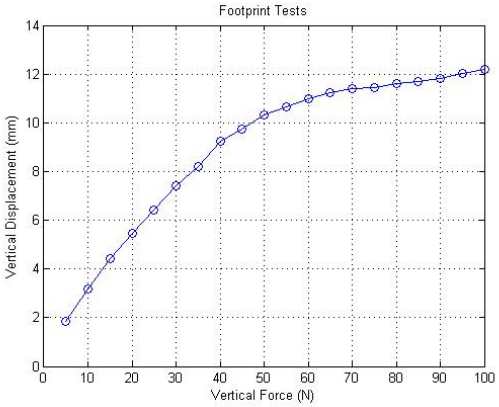

Figure 4: Footprint tests: Vertical displacement versus Vertical force.

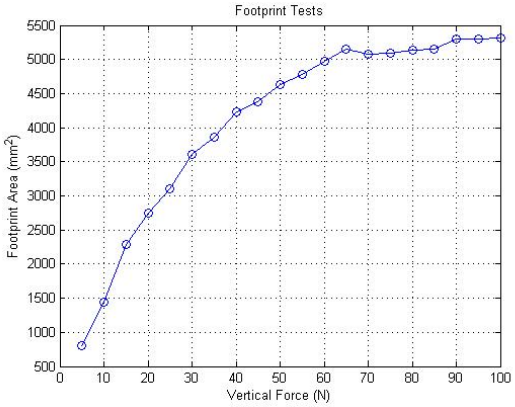

Figure 5: Footprint tests: Footprint area versus Vertical force.

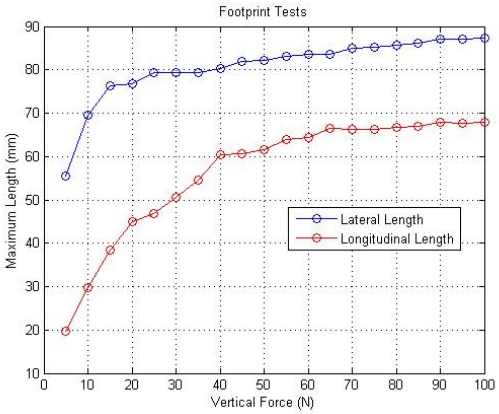

Figure 6: Footprint tests: Maximum length versus Vertical force.

driven by the fact that this is a reasonable loading for small to medium-sized robots and by the available space inside the tyre. With this placement, it is ensured that all the sensors are located inside the area of the contact patch under all possible loading conditions. Choosing a smaller area, such as the footprint of 5 N, was not possible due to physical limitations where, in such a small area, the sensors would have to be stacked close to each other. With the used strain gauges, this is not possible since these standard, low-cost sensors require delicate operation of gluing and soldering. In addition, this would have resulted in no significant differences in the readings of the sensors since they would be located in the same limited space. Finally, since the sensors are inside the contact patch when 10N vertical load is applied, they will certainly be within the contact patch when bigger loads are exerted.

To decide the most appropriate sensor system design for the used tyre, some criteria were placed. Most importantly, it must be able to capture measurements reflecting the strain distribution in both longitudinal and lateral directions. The reason for that was to cover the possible cases of tyre braking, traction, and turning (cornering). Other factors which affected the decision were the tyre's small size, the minimum number of required sensors, and the best locations to position the sensors. Hence, the design explained in this section was judged to be the most promising configuration.

Regardless of the shape of the contact patch, the circumferential (longitudinal) strain can be measured with one sensor placed longitudinally on the centreline, i.e., at the middle of the contact patch. Even under braking or traction, one circumferential sensor placed at the centreline is enough to measure the corresponding change in the circumferential strain distribution. In contrast, two sensors placed laterally and symmetrically about the centreline are required to measure the change in the axial (lateral) strain distribution. These two lateral sensors give different measurements during steering (cornering) because they capture the asymmetric lateral strain distribution [Yang, 2011].

In the selected design, six strain gauges were glued on the tyre inner surface as illustrated in Figure 7. In details, the implemented design consists of three pairs of strain gauges where, in each pair, one strain gauge is placed longitudinally while the other is placed laterally with respect to tyre direction of rotation. One pair is mounted on the tyre centreline while the other two pairs are placed symmetrically about the centreline. If higher data update rate is required, this design can be repeated circumferentially, for example, it could be located at $120°$, $0°$, and $-120°$. Considering the previous points related to placing longitudinal and lateral sensors, it can be concluded that the proposed design contains three redundant sensors, two side longitudinal sensors and one middle lateral sensor. The reasons for that was to account for possible misalignments in sensors mounting as well as different degrees of thickness across the tyre due to tread pattern. In addition, distributing the sensors

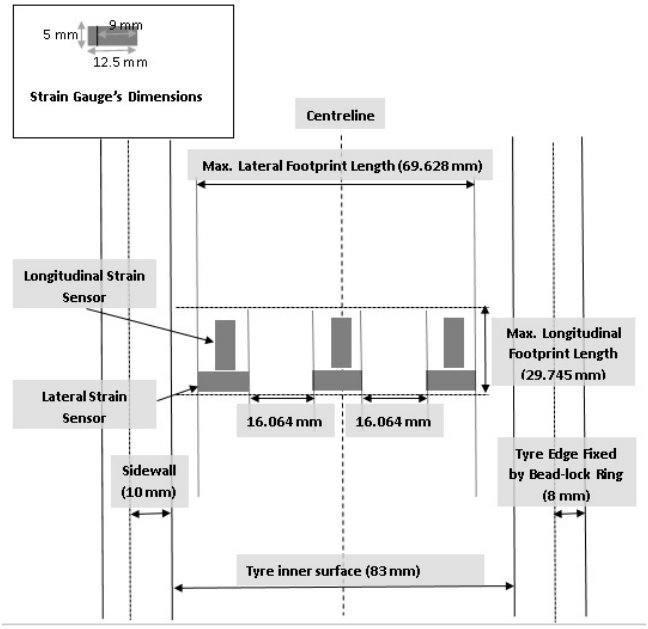

Figure 7: Sketch of tyre inner surface with the sensor system design.

across the tyre width is useful in obtaining the contact shape information.

Lastly, it can be mentioned that some previous works suggested that placing sensors on the tyre sidewall might give useful information which could complement the readings collected from the tyre tread. However, with the used tyre, where the sidewall is very small (less than 10 mm), it is physically very difficult to put a sensor that would operate properly. Some of the main issues would be the small space where the sensor is supposed to be glued, high probability of sensor debonding, soldering, and wiring.

5.2 Sensor System's Placement

This process involved three stages: bonding the design to the tyre inner surface, soldering wires to the gauges, and assembling the wheel. The following operations were performed to prepare the tyre inner surface for the bonding stage. First, degreasing an area which is bigger than that needed for the sensor system placement using isopropyl alcohol and gauze swabs. Then, abrading the same area using 320-grit abrasive paper. After that, removing residuals from the abrasion operation using alcohol and gauze. Finally, marking the tyre centreline near the area.

To build the sensor system, six strain gauges were prepared. The following steps were followed. A paper with the desired sensor design, as in Figure 7, where the exact positions of the sensors are shown, was attached to the bottom side of a glass board which will be the work surface. After that, the gauges were transferred to the glass board and, using the diagram on the paper attached to the glass board, they were positioned to their suggested locations in the design. Lastly, a piece of wide sticky tape was used to transfer all the gauges at once to the tyre inner surface.

To glue the sensors, the sticky tape holding the gauges was fixed to the tyre inner surface such as the sensors are positioned to their correct locations. To do so, the marks drawn on the tyre inner centreline were used as a reference. Next, the design was mounted on the tyre inner surface with three consecutive steps. In each step, part of the sticky tape was lifted to glue the two sensors, one longitudinal and one lateral, which are close to each other. Then, an enough amount of adhesive (alkayl glue) was placed on the tyre and then the sensors were aligned back on their positions on the tyre. Figure 8 shows the sensor system design glued to the tyre inner surface.

The second stage was soldering wires to the gauges. Figure 9 shows the sensor system after the soldering process.

The Final step was assembling the tyre, foam, and wheel together. To do this, two holes were created in the foam to pass the wires from inside the tyre to outside the foam. Then, two existing holes in the wheel were used to pass the wires as shown in Figure 10(a). Then, the foam was carefully inserted inside the tyre as shown in Figure 10(b) and, finally, the wheel was placed inside the tyre and foam assembly as shown in Figure 10(c). The tyre was then fixed to the rim using the two rim lock rings.

6 Experimental Results and Discussion

The bench-top rig presented earlier was modified to allow measuring tyre strains at different angular positions. As can be seen in Figure 11, a purpose-built clamp, which was fixed at one end to the wheel using four screws in

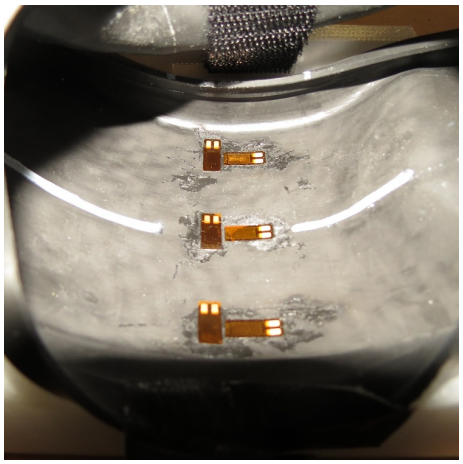

Figure 8: The sensor system glued to the tyre inner surface.

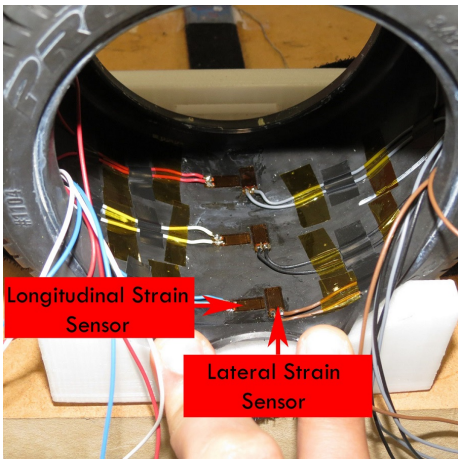

Figure 9: The sensor system after the soldering process.

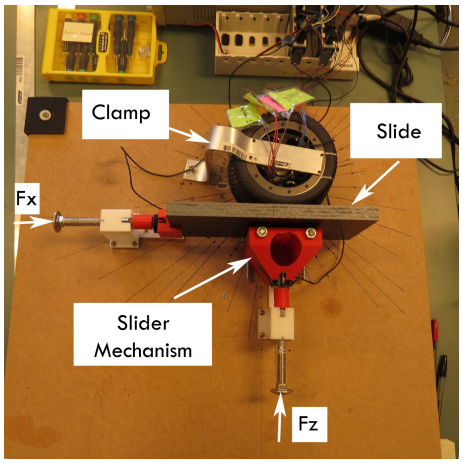

Figure 11: Tyre bench-top rig used for static tests.

the bead-lock rim and was screwed at the other end to the board, was used to hold the tyre at different angles. Thus, static tests with different vertical forces, horizontal forces, and sensors' angular positions were conducted. In the following, pieces of evidence that the sensing system is working will be presented.

Figure 12 shows an example of strain profiles measured by the sensors. This figure illustrates that the strain profiles produced by the three longitudinal sensors convey similar features in terms of waveform shapes and strain variations at angular positions. This similarity is more perceptible in the readings of the two side sensors, named longitudinal 1 and longitudinal 3. This is related to the fact that these two sensors are mounted in the same spot on the two opposite sides. As a result, they stretch in the same manner in response to the applied forces and thus they give comparable results. This observation is also true for the readings of the lateral sensors. In the same context, it is worth mentioning that there are no clear similarities between the longitudinal sensors' readings and the lateral sensors' readings. This is because the former indicates strains caused by stretching of the tyre in a direction parallel to the direction of the application of the horizontal force while the latter records strains caused by stretching in a direction perpendicular to the horizontal force. From these comparisons, it can be concluded that the embedded strain gauges are working properly since their readings are related to their position and orientation.

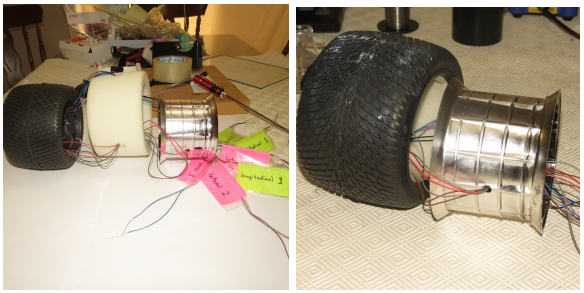

(a) (b)

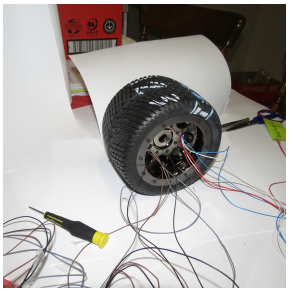

(c)

Figure 10: Assembling the wheel: (a) step 1, (b) step 2, (c) step 3.

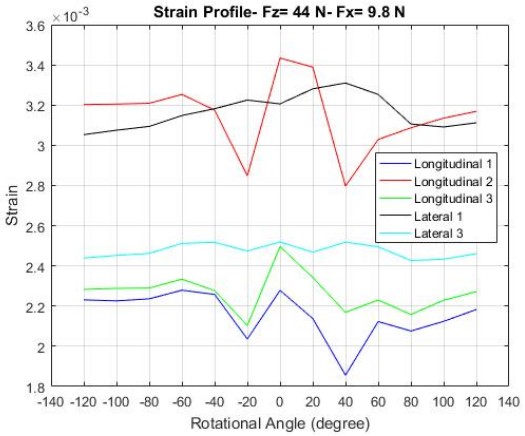

Figure 12: Example of a strain profile collected by the strain gauges. Lateral 2 is not presented because it has malfunctioned

In Figure 12, assuming that angle 0° is the centre of

the contact patch, slight changes in strain values are noticed in the angles far from the contact patch at both sides, i.e., angles $-120°$ to $-60°$ and $60°$ to $120°$. On the contrary, such variations become more significant in the vicinity of the contact patch, namely, at angles $-60°$ to $60°$. Same observations about strain changes were reported by Yang [2011]. These strain variations are attributed to corresponding deformations around tyre circumference. The part of the tyre which makes contact with the ground is the most deformed since it endures effects of applied vertical and horizontal forces. Therefore, the strain changes are higher in this area.

Figure 12 indicates that the tyre is stretching in one direction at some of the angles whereas it stretches in the opposite direction (compresses) at other angles. For the three longitudinal sensors, it can be seen that tensile strain is recorded at the centre of the contact patch while compressive strains are noticed in nearby regions at the two sides of the contact centre, i.e., around $\pm 20°$. This agrees with results presented by Matsuzaki and Todoroki [2008]. For the lateral sensors, the lateral strain profile shows features which are the opposite of those for the longitudinal strain profile. This behaviour is especially observable in the readings of the sensor called lateral 1. Therefore, the tyre is under tensile lateral strain both before and after the contact region while it is under compressive lateral strain within this region. The same conclusion regarding lateral strains is reported by Yang [2011].

Figure 13 and Figure 14 shows an example of the relationship between the horizontal force (Fx) and the strain at a constant value of the vertical force (Fz) at each of the tested angular positions for a longitudinal and a lateral sensor, respectively. Figure 15 and Figure 16 shows an example of the the relationship between Fz and the strain at a constant value of Fx at each of the tested angular positions for a longitudinal and a lateral sensor, respectively. It can be seen in these figures that the sensors' readings demonstrate linear relationship between the applied force, horizontal or vertical, and the strain values. In addition, the graphs show that the lines representing the relationships are evenly spaced and close to each other which indicates a consistent performance for the sensors.

Figure 13- Figure 16 show that as the sensors become closer to the contact patch, the slope of the lines becomes steeper. This is because the strain at the points near and in the contact patch is higher. Consequently, increasing the applied force results in larger changes in strain magnitudes at these points as compared to those at the angles which are far from the contact patch.

From the readings of the longitudinal sensor in Figure 15 , it is seen that increasing the value of Fz causes a decrease in the strain value.

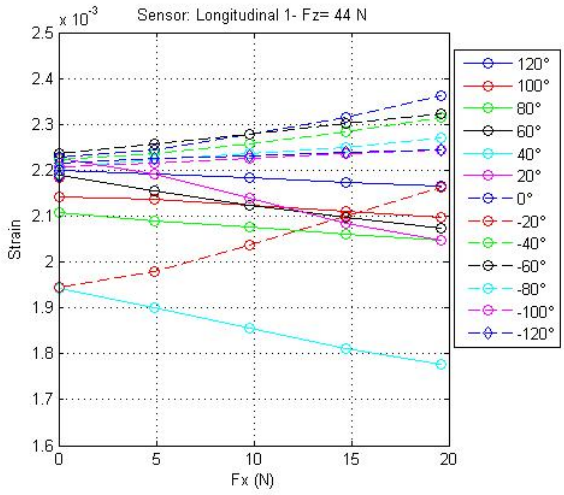

Figure 13: Strain versus Fx at tested angles (Example: Sensor- Longitudinal 1).

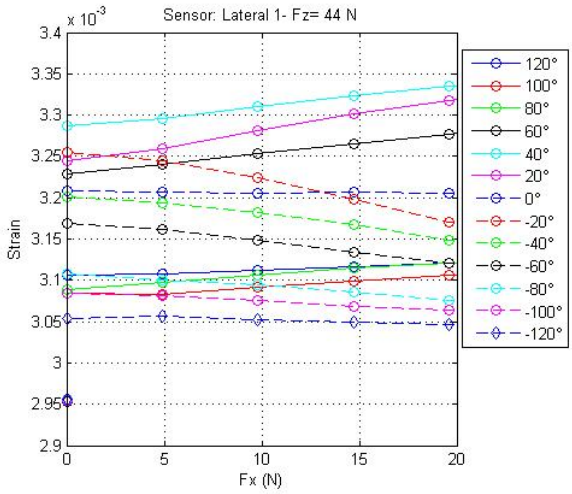

Figure 14: Strain versus Fx at tested angles (Example: Sensor- Lateral 1).

In contrast with the longitudinal sensors, readings from the lateral sensor shown in Figure 16 demonstrate that as the value of Fz increases, the strain value increases. This response of longitudinal and lateral sensors to increasing Fz is also seen in results introduced by Yang [2011].

Lastly, it is worthwhile mentioning that the strain profiles shown in Figure 12 can be used to estimate the applied forces and the slip ratio. The average of the strain peaks existed in these profiles are related to the vertical force while the ratio of these peaks correponds to the horizontal force [Yang, 2011]. In addition, these profiles can be differentiated to estimate the contact patch edges, centre, and length. Thus, an alternative method can be used to estimate the forces. To clarify, the contact

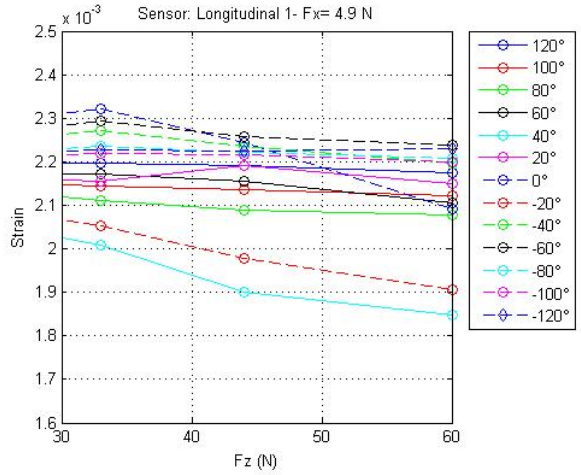

Figure 15: Strain versus Fz at tested angles (Example: Sensor- Longitudinal 1).

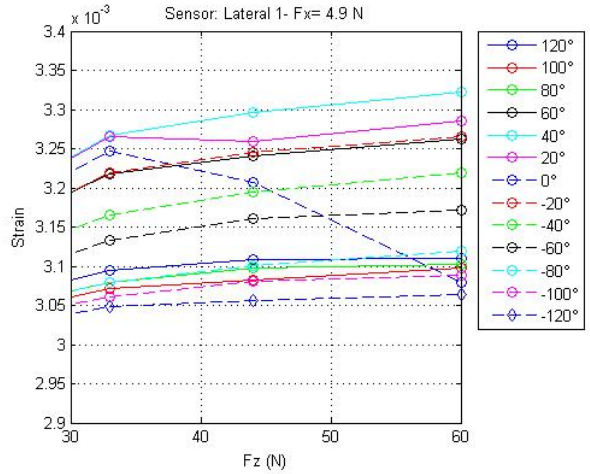

Figure 16: Strain versus Fz at tested angles (Example: Sensor- Lateral 1).

patch length corresponds to the vertical load whereas the shift in the contact centre is related to the horizontal force [Krier *et al.*, 2014]. Furthermore, the contact patch length is also linearly and inversely proportional to the effective radius. Therefore, the contact patch length is used to derive the effective radius. Then the value of the estimated effective radius is inserted into the following equation to calculate the slip ratio [Matsuzaki and Todoroki, 2008]:

$$s = \frac{V - \omega r_e}{V} \tag{1}$$

Where (V) is the robot's linear velocity, (ω) represents the wheel angular velocity, and (r_e) is the effective radius.

7 Conclusion and Future Work

This paper has showed the initial results of the first step in building a tyre strain sensing system for the slip estimation in a small, non-pressurised tyre. It has presented a modern sensing technique, which utilizes sensors mounted inside tyres, to directly monitor the tyre-ground interactions. A comprehensive study of in-tyre sensing systems led to selecting a contacting strain sensing system for the robot's tyre used in this research. Experimental work was conducted to examine possible techniques of mounting this system inside a small, non-pressurised tyre. After that, static footprint tests were utilised to study the tyre-ground contact area and suggest a sensor system design. Next, the implemented design was tested through static tests using a bench-top rig. These tests showed promisimg results because they indicated consistent performance by the sensors. Also, the tests illustrated that the design delivers reasonable and expected output which agrees with work of previous researchers. Future work will focus on developing a deeper analysis for the results of these static tests to extract useful information for wheel slip estimation. Later on, advanced, dynamic tests will be undertaken to evaluate the performance of the sensor design and the slip estimation method in various working conditions.

Acknowledgments

This work has been supported by the University of Southern Queensland. The senior author would like to acknowledge the University of Technology, Baghdad, Iraq for funding the PhD scholarship.

References

[Chae and Song, 2013] Heewon Chae and Jae-Bok Song. Slippage detection and pose recovery for upward-looking camera-based slam using optical flow. In *13th International Conference on Control, Automation and Systems (ICCAS)*, pages 1108–1113, Gwangju, Korea, 20-23 October 2013.

[Erdogan *et al.*, 2011] Gurkan Erdogan, Lee Alexander, and Rajesh Rajamani. Estimation of tire-road friction coefficient using a novel wireless piezoelectric tire sensor. *IEEE Sensors Journal*, 11(2):267–279, 2011.

[Ergen *et al.*, 2009] Sinem Coleri Ergen, Alberto Sangiovanni-Vincentelli, Xuening Sun, Riccardo Tebano, Sayf Alalusi, Giorgio Audisio, and Marco Sabatini. The tire as an intelligent sensor. *IEEE Transactions on Computer-Aided Design of Integrated Circuits and Systems*, 28(7):941–955, July 2009.

[Iizuka *et al.*, 2014] Kojiro Iizuka, Tatsuya Sasaki, Mitsuhiro Yamano, and Takashi Kubota. Development of

grousers with a tactile sensor for wheels of lunar exploration rovers to measure sinkage. *International Journal of Advanced Robotic Systems*, 11(49):1–7, 2014.

[Ise *et al.*, 2013] Taisei Ise, Masahiro Higuchi, and Hiroshi Tachiya. Development of a tactile sensor to measure tire friction coefficients in arbitrary directions. *International Journal of Automation Technology*, 7(3):359– 366, 2013.

[Krier *et al.*, 2014] David Krier, Gabriele S. Zanardo, and Luigi del Re. A pca-based modeling approach for estimation of road-tire forces by in-tire accelerometers. In *19th World Congress, The International Federation of Automatic Control (IFAC)*, pages 12029–12034, Cape Town, South Africa. 24-29 August 2014.

[Magori *et al.*, 1998] Valentin Magori, Valentin R. Magori, and N. Seitz. On-line determination of tyre deformation, a novel sensor principle. In *IEEE Proceedings of Ultrasonics Symposium*, pages 485–488, Sendai, Japan, 1998.

[Matsuzaki and Todoroki, 2008] Ryosuke Matsuzaki and Akira Todoroki. Intelligent tires based on measurement of tire deformation. In *Journal of solid mechanics and Materials engineering*, 2(2):269–280, 2008.

[Matsuzaki *et al.*, 2012] Ryosuke Matsuzaki, Naoki Hiraoka, Akira Todoroki, and Yoshihiro Mizutani. Strain monitoring and applied load estimation for the development of intelligent tires using a single wireless ccd camera. *Journal of Solid Mechanics and Materials Engineering*, 6(9):935–949, 2012.

[Moffitt *et al.*, 2009] Ronald D. Moffitt, Scott M. Bland, Mohammad R. Sunny, and Rakesh K. Kapania. Sensor technologies for direct health monitoring of tires. *Encyclopedia of Structural Health Monitoring*, John Wiley Sons, Ltd., ISBN: 978-0-470-05822-0, 2008.

[Palmer *et al.*, 2002] Matthew E. Palmer, Clark C. Boyd, Jim McManus, and Scott Meller. Wireless smart tires for road friction measurement and self state determination. In *43rd AIAA/ASME/ASCE/AHS Structures, Structural Dynamics, and Materials Conference*, Paper AIAA-2002-1548, Denver, Colorado, 22-25 April 2002.

[Song *et al.*, 2008] Xiaojing Song, Zibin Song, Lakmal D Seneviratne, and Kaspar Althoefer. Optical flow-based slip and velocity estimation technique for unmanned skid-steered vehicles. *IEEE/RSJ International Conference on Intelligent Robots and Systems*, pages 101–106, Nice, France, 22-26 September 2008.

[Tuononen, 2008] A.J. Tuononen. Optical position detection to measure tyre carcass deflections. *Vehicle System Dynamics*,46(6):471–481, 2008.

[Ward and Iagnemma, 2008] Chris C. Ward and Karl Iagnemma. A dynamic-model-based wheel slip detector for mobile robots on outdoor terrain. In *IEEE Transactions on Robotics*, 24(4):821–831, 2008.

[Xiong and Tuononen, 2014] Yi Xiong and Ari Tuononen. A laser-based sensor system for tire tread deformation measurement. *Measurement Science and Technology*, 25(11), 115103, 2014.

[Yang, 2011] Yang X. *Finite element analysis and experimental investigation of tyre characteristics for developing strain-based intelligent tyre system.* Ph.D. dissertation, Dept. Mech. Eng., The University of Birmingham, Birmingham, UK, September 2011.

[Yi, 2008] Jingang Yi. A piezo-sensor-based smart tire system for mobile robots and vehicles. In *IEEE/ASME Transactions on Mechatronics*, 13(1):95–103, February 2008.

[Yi *et al.*, 2009] Jingang Yi, Hongpeng Wang, Junjie Zhang, Dezhen Song, Suhada Jayasuriya, and Jingtai Liu. Kinematic modeling and analysis of skid-steered mobile robots with applications to low-cost inertial-measurement-unit-based motion estimation. In *IEEE Transactions on Robotics*, 25(5):1087–1097, October 2009.

[Zhang *et al.*, 2013] Yizhai Zhang,Jingang Yi, and Tao Liu. Embedded flexible force sensor for in-situ tire-road interaction measurements. *IEEE SENSORS JOURNAL*, 13(5):1756–1765, May 2013.